J. Membrane Biol. 125, 81–91 (1992)

The Journal of
Membrane Biology
© Springer-Verlag New York Inc. 1992

Evidence that Plasma Membrane Electrical Potential Is Required for Vesicular Stomatitis Virus Infection of MDCK Cells: A Study Using Fluorescence Measurements through Polycarbonate Supports

Mark Akeson, Joshua Scharff, Celia M. Sharp, and David M. Neville, Jr.
Laboratory of Molecular Biology, Section on Biophysical Chemistry, National Institute of Mental Health, Bethesda, Maryland 20892

Summary. We used fluorescence microscopy of Madin-Darby Canine Kidney (MDCK) cells grown on polycarbonate filters to study a possible link between plasma membrane electrical potential ($\Delta\Psi_{pm}$) and infectivity of vesicular stomatitis virus (VSV). Complete substitution of K^+ for extracellular Na^+ blocks VSV infection of MDCK cells as well as baby hamster kidney (BHK) cells. When we independently perfused the apical and basal-lateral surfaces of high resistance monolayers, high K^+ inhibited VSV infection of MDCK cells only when applied to the basal-lateral side; high K^+ applied apically had no effect on VSV infection. This morphological specificity correlates with a large decrease in $\Delta\Psi_{pm}$ of MDCK cells when high K^+ buffer is perfused across the basal-lateral surface. Depolarization of the plasma membrane by 130 mM basal K^+ causes a sustained increase of cytosol pH in MDCK cells from 7.3 to 7.5 as reported by the fluorescent dye BCECF. Depolarization also causes a transient increase of cytosol Ca^{2+} from 70 to 300 nM as reported by the dye Fura-2. Neither increase could explain the block of VSV infectivity by plasma membrane depolarization. One alternative hypothesis is that $\Delta\Psi_{pm}$ facilitates membrane translocation of viral macromolecules as previously described for colicins, mitochondrial import proteins, and proteins secreted by *Escherichia coli*.

Key Words membrane potential · vesicular stomatitis virus · MDCK · calcium · pH

Introduction

Acid-processed enveloped viruses infect cells *via* endocytic pathways. It is generally observed that raising the pH of the endosomal lumen by addition of ammonia or monensin prevents pH-dependent fusion between membranes of these viruses and endosomal membranes (Marsh & Helenius, 1989). This acid dependence is best understood for influenza virus, where low pH is known to trigger a conformational shift in a membrane glycoprotein that mediates membrane fusion (Wiley & Skehel, 1987).

Helenius and coworkers (1985) discovered another mechanism that blocks infection by one member of this class of viruses, Semliki Forest virus (SFV). Using BHK cells grown on glass, they found that infection was prevented in low Na^+ media. The effect was not ion specific, but instead correlated with an apparent decrease in plasma membrane electrical potential ($\Delta\Psi_{pm}$). The exact step in the viral infection process requiring $\Delta\Psi_{pm}$ was not identified but it appeared to be an early event. Viral membrane-endosomal membrane fusion was proposed as a possibility (Helenius et al., 1985).

The most plausible cause of the depolarization observed by Helenius and co-workers (1985) was the isosmotic substitution of KCl for NaCl. Concentration-driven K^+ efflux from cytosol through K^+-selective channels contributes significantly to plasma membrane potential in a variety of cells, including epithelial cells (Paulmichl, Gstraunthaler & Lang, 1985). Thus, substitution of K^+ for Na^+ in the external buffer would be expected to decrease the concentration gradient responsible for generating plasma membrane potential and might thereby inhibit infection. One objective of this study was to examine this link between extracellular K^+, $\Delta\Psi_{pm}$, and infectivity of another acid-processed enveloped virus, VSV. Another objective was to determine if plasma membrane depolarization can induce shifts of cytosol Ca^{2+} or pH, and if so, whether or not either shift could explain inhibition of infection. We are particularly interested in this question because one long-range goal of our laboratory is to determine if depolarization blocks infection through a cytosolic second messenger—e.g., Ca^{2+}—or whether the block occurs at the plasma membrane *per se*. For example, one hypothesis is that $\Delta\Psi_{pm}$ is used to insert a component of the viral nucleocapsid into

the plasma membrane in a manner similar to $\Delta\Psi_{pm}$-dependent insertion of a segment of the E1 colicin channel (Merrill & Cramer, 1990; Abrams et al., 1991).

We found that high K^+ media inhibit VSV infection of both BHK cells and polarized MDCK cells, and that inhibition only occurs when high K^+ buffer is applied to the basal-lateral membrane of the polarized cell line. We also found that depolarization caused increases of $[Ca^{2+}]_i$ and pH_i, but neither shift contributed to inhibition of infection.

Materials and Methods

MDCK Cell Culture and Cloning

MDCK II cells (American Type Culture Collection stock no. CCL34) were maintained in a modified minimum essential Eagle's solution (Flow Laboratories, McLean, VA) supplemented with 25 mM sodium bicarbonate, 100 units ml^{-1} penicillin-streptomycin (Advanced Biotechnologies, Columbia, MD) and 10% (vol/vol) fetal bovine serum. The cells were passed seven times and then cloned using the infinite dilution method. This resulted in two types of cells distinguished by monolayer resistance measured with a World Precision Instruments EVOM ohmmeter: MDCK-CC 101891 A-11 (R_{max} = 4200 Ω cm^2) and MDCK-CC 101891 G-11 (R_{max} = 110 Ω cm^2). The high resistance clone was used in this study.

Polarized monolayers were formed by seeding MDCK A-11 cells on Costar Transwell polycarbonate inserts (6.5-mm diameter; 3.0-μm pore diameter) at 2×10^4 cells $well^{-1}$ and growing them to confluency in the same medium as above at 37°C in a 5% CO_2 hydrated atmosphere. These cells were used up to seven days after seeding. Monolayer resistance peaked at three days post-seeding then declined gradually. Resistance always exceeded 500 Ω cm^2.

Protein Synthesis Assay

Protein synthesis of MDCK monolayers in Transwells, following exposure to depolarizing agents, was measured relative to controls by pulsing the basilar compartment with ^{14}C-L-leucine. A pre-addition pulse with ^{3}H-L-leucine was also performed as an internal control and served to correct for variations in control protein synthetic rates and cell harvesting. Cell protein was harvested onto filter pads using a Skatron harvester (Sterling, VA) with a 12-channel head following a brief exposure of basal and apical chambers to 0.1 mM EDTA at pH 7.4. Dried filters were counted in Ecolume (ICN, Costa Mesa, CA) on a Beckman LS 2800 Scintillation Counter using narrow ^{3}H (0–280) and ^{14}C (400–670) windows to eliminate significant spillover.

VSV Infection Assay

MDCK cells grown on 3.0-μm pore size Costar polycarbonate filters were used 3–4 days post-seeding. At the beginning of each experiment, monolayers were rinsed three times at 37°C in buffer 'A' supplemented with 0.1% bovine serum albumin. Buffer A was composed of minimum essential medium (MEM) modified with 25 mM HEPES/NaOH (pH 7.4), MEM nonessential amino acids, 100 units ml^{-1} penicillin, 100 μg ml^{-1} streptomycin, and 0.2 g $liter^{-1}$ (2.4 mM) $NaHCO_3$. In the standard formulation used here, this buffer contained 130 mM Na^+ and 5 mM K^+. Any increase in K^+ concentration of this buffer for an experiment was balanced by an equimolar decrease in Na^+ to maintain constant osmolarity. Thus the statement 'high K^+' in this report implies low Na^+. The cells were gradually cooled to 5°C and then placed on ice for 15 min. 1×10^7 plaque forming units (PFU) $well^{-1}$ of VSV (Indiana serotype) were added to the monolayers and incubated (ice cold) for 30 min to allow surface binding of the virus. The cells were then warmed to 37°C in a 1% CO_2 incubator for 5 min to allow endocytosis, and subsequently, transferred to experimental media containing a 1:50 dilution of anti-VSV (Lee Biomolecular Research, San Diego, CA, cat. no. 06141) and incubated for 160 min at 37°C under 1% CO_2. At 160 min, all treatments were rinsed three times in buffer A to remove anti-VSV, and the incubation was continued for the virus plaque assay.

The BHK infection assay was performed in essentially the same way except that cells were grown to confluency in 24 plates rather than in Transwell inserts, and the buffer used during the experiment was standard MEM (pH 7.4) at 5% CO_2. Experiments with added $BaCl_2$ were performed in buffers that contained no $NaHCO_3$ to prevent barium carbonate precipitation.

Plaque Assay

At various times up to 8 hr, aliquots were removed from the treatments and tested for virions by a conventional plaque assay. Briefly, BHK cells were grown to confluency in 24-well plates (Flow Laboratories, McLean, VA) containing EMEM. One hundred μl of dilute virus suspension in buffer A was added per well and incubated for 30 min at 37°C under 1% CO_2, with occasional agitation to prevent cell dessication. Unbound virus was removed by aspiration, and 1 ml EMEM (without phenol red) containing 0.9% (wt/vol) warm agarose was added. The gel was then incubated for 24 hr at 37°C and 5% CO_2. At 24 hr, 1 ml of the same medium plus 83 mg $liter^{-1}$ neutral red was added, and the incubation continued. Plaques were counted within 24 hr.

Fluorescence Microscopy

We used 3-μm pore size Costar Transwell inserts in this study. This 10-μm thick polycarbonate filter appears translucent to the naked eye although back scattering of light is evident. This is in contrast to the more commonly used 0.45-μm pore size filter which appears opaque. Inserts supporting MDCK monolayers ($R > 500$ Ω cm^{-2}) were placed upon two 20-μm thick flat glass capillaries (Vitro Dynamics, Rockaway, NJ) that ran parallel, 5 mm apart, atop a number 0 glass coverslip (Biophysica Technologies, Baltimore, MD) held in a Leiden coverslip dish (Medical Systems, Greenvale, NY). Buffer was delivered independently through Teflon tubing to the apical and basal-lateral surfaces from two syringe pumps (Orion, Boston, MA) at 0.2 ml min^{-1} each. To ensure that buffer reached the basal-lateral surface efficiently, a borosilicate glass pipette was attached to the basal-lateral perfusion tube so that its 20-μm diameter tip nested beneath the Transwell filter and between the glass capillaries. Unless otherwise noted, the temperature of the perfusate delivered to the cells was controlled at 37 ± 0.5°C by passing it through Teflon tubing coiled in a Peltier device (PDMI-2, Medical Systems, Greenvale, NY). A mixture of 1% CO_2 and 99% air was warmed in the Peltier device and passed continually over the surface of the bath.

Fura-2 and BCECF (2',7'-bis-(2-carboxyethyl)-5-(and-6)carboxyfluorescein) (Molecular Probes, Eugene, OR) were loaded into MDCK cells as follows. MDCK monolayers on Transwell inserts were washed three times in buffer A, then equilibrated in a 1% CO_2 atmosphere at 37°C for 2 hr. They were then incubated under the same conditions for 30 min in buffer A supplemented (per ml) with 2 μl of 1 mM Fura-2-AM (the membrane-permeant acetoxymethyl ester of Fura-2) or 1 mM BCECF-AM (the acetoxymethyl ester of BCECF) in DMSO, 4 μl of DMSO, and 250 μM sulfinpyrazone (Sigma, St. Louis, MO) to block rapid unloading of the de-esterified dyes from cytosol (Di Virgilio, Steinberg & Silverstein, 1990). Unless otherwise noted, all buffers contained sulfinpyrazone for the duration of any experiment where cells had been loaded with BCECF or Fura-2. Following dye loading, the cells were washed twice in buffer A and then placed onto the microscope. DiBAC(4)$_3^-$(bis(1,3-dibutyl-barbituric acid-(5))trimethineoxonol) was loaded into MDCK cells by perfusing them for 20 min at 37°C in buffer A, modified to contain 90 mM Na^+ and 45 mM K^+, followed by 20 min perfusion in buffer A.

Cells were viewed with an inverted epifluorescence microscope mounted on a vertical optical bench (Yona Microscope & Instrument, Silver Spring, MD) through a Nikon 40X/1.3 NA CF Fluor DL objective lense mounted on top of a Leitz Ploempack fluorescence accessory. The excitation light source was a 100-W mercury short-arc lamp with an Oriel model 68830 power supply and model 68850 photofeedback unit. Excitation light was filtered alternately at 340 and 380 nm (Fura-2) or at 495 and 440 nm (BCECF) by a computer-controlled stepping motor. For DiBAC(4)$_3^-$, the excitation frequency was maintained at 495 nm. Light emitted from the samples was passed through filter cubes held in the Ploempack. The emission cubes (and their associated excitation filters) were specifically designed for fluorescence measurements with Fura-2 (400-nm dichroic, 510-nm long-pass filter) or BCECF (515-nm dichroic, 535-nm long-pass filter) (Omega Optical, Brattleboro, VT). The BCECF cube was also suitable for DiBAC(4)$_3^-$ measurements. The filtered intermediate image of the objective was placed at the input of a microchannel plate intensifier (Model KS-1380, Video Scope International, Washington, D.C.), which was coupled by 85-mm f 2.0 and 50-mm f 1.2 camera lenses (Olympus) to a CCD camera (Video Scope International, Model CCD 200E). This configuration minimized magnification resulting in x-axis magnification of 0.52 μm per pixel.

Images were digitized as 512 × 512 × 8 bits and averaged (eight frames per time point) in a Trapix 55/4256 image processor and stored in VisiStore (Recognition Concepts, Incline Village, NV). Nonaveraged images could be acquired at 15 frames sec^{-1}, and a total of 2466 images could be stored. For each time point, BCECF or Fura-2 fluorescence intensity ratios were calculated pixel by pixel from intensities for the two excitation wavelengths. The DiBAC(4)$_3^-$ fluorescence signal could not be normalized. Regions of interest within the visible field—either single cells or groups of ten cells—were then selected with a box cursor and by grey level thresholding. In this study autofluorescence from the sample or optical components and back-scattered exciting light were not significant. Consequently, single wavelength images were not corrected by blank subtraction. Data in this report represent either the mean fluorescence ratio within a region of interest or the light intensity (grey level) for a single wavelength. Software for image acquisition, image processing, and importation into graphics programs was designed in house with the aid of Synergistic Research Systems, Silver Spring, MD.

The ratio of BCECF fluorescence at 495- *vs.* 440-nm excitation frequency was calibrated against intracellular pH by treating BCECF-loaded MDCK cells with 10 μM nigericin and 5 μM valinomycin in buffer A containing 130 mM K^+ and 5 mM Na^+. The cells were then perfused with the same buffer at pH values from 6.0 to 7.8 from which a calibration curve could be generated. Intracellular Ca^{2+} concentration $[Ca^{2+}]_i$ was calculated from the Fura-2 fluorescence ratio ($R = F_{340}/F_{380}$) using the following equation (Grynkiewicz, Poenie & Tsien, 1985)

$$[Ca^{2+}]_i = K_d[(R - R_{min})/(R_{max} - R)]\beta$$

where K_d = 135 nM (Fatatis & Russell, 1991), $R_{min} = F_{340}/F_{380}$ at 10^{-11} M Ca^{2+}, $R_{max} = F_{340}/F_{380}$ at 10^{-3} M Ca^{2+}, $\beta = F_{380}$ at 10^{-11} M Ca^{2+}/F_{380} at 10^{-3} M Ca^{2+}, and F_{340} and F_{380} equal fluorescence intensities at 340- and 380-nm excitation frequencies, respectively. R_{min} and R_{max} were measured by perfusing Fura-2-loaded MDCK cells with 130 mM K^+/5 mM Na^+ buffer A containing 5 μM ionomycin and either 1.8 mM Ca^{2+} (R_{max}) or 10 mM EGTA + 1.8 mM Ca^{2+} (R_{min}).

Results

High K^+ Media Inhibit VSV Infection of BHK Cells

The time course of a typical VSV infection assay using BHK cells is shown in Fig. 1*a*. Addition of 145 mM K^+ after endocytosis (5 to 180 min) dropped virus production 560-fold compared to production in standard EMEM (140 mM Na^+, 5 mM K^+) (Fig. 1*b-c*). By comparison, addition of high K^+ medium during surface binding and endocytosis (−20 to 5 min) had no effect on VSV infection (*data not shown*). Thus, substitution of K^+ for Na^+ in the external buffer inhibits VSV infection of BHK cells at a step following endocytosis as is true for SFV infection (Helenius et al., 1985).

We wished to narrow the time frame when post-endocytic inhibition of VSV synthesis occurred. Figure 1*d* and *e* shows results for cells treated as in Fig. 1*c* except that standard 140-mM Na^+, 5 mM K^+ medium was applied to the cells from 5–12 or 5–24 min. The high Na^+ window from 5–12 min permitted some recovery of virus synthesis (190-fold less than control), and the 5–24 min high Na^+ window gave marked recovery (14-fold less than control). We conclude that the major K^+-sensitive step occurs within the first 20 min of virus synthesis following endocytosis in BHK cells.

Fluorescence Measurements Through 3.0-μm Pore Size Polycarbonate Filters

One tool we used in this study was fluorescence microscopy of high resistance MDCK cells grown on permeable supports as diagrammed in Fig. 2. Because this set-up combined two procedures for the first time—i.e., independent perfusion of the apical and basal-lateral membranes and measure-

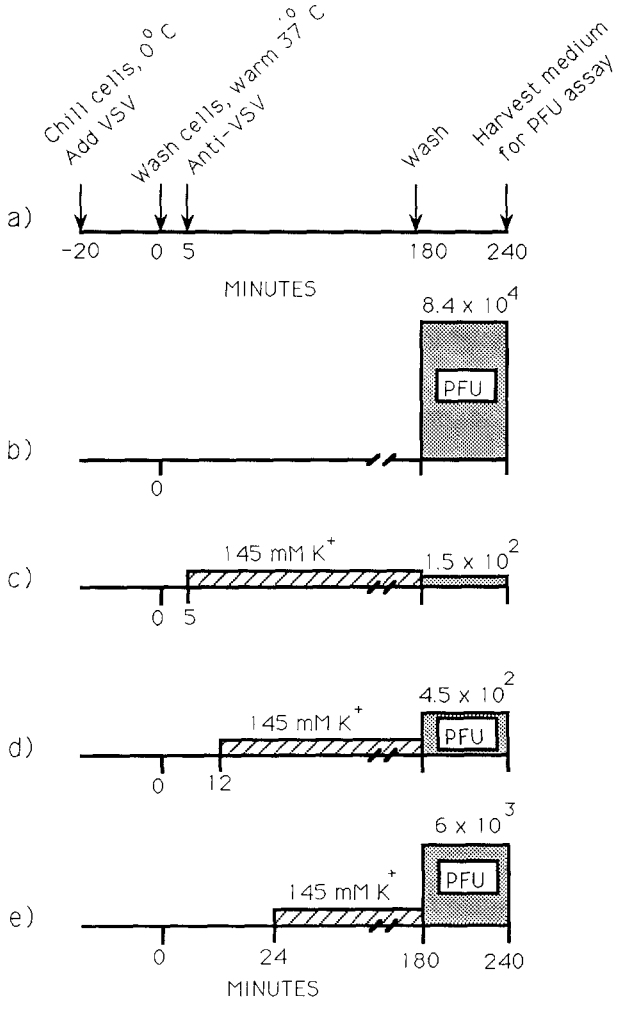

Fig. 1. The effect of high K^+ media on VSV production in BHK cells. (*a*) Steps involved in the experiment as described in Materials and Methods. (*b*) A control in which cells were incubated in standard MEM at 37°C under 5% CO_2 for the duration of the experiment. (*c*)–(*e*) Identical to the control except that cells were bathed in 145 mM K^+ MEM for the times shown. At 180 min, each well was rinsed three times in MEM to remove anti-VSV so that viruses that budded from the BHK cells would remain viable. The incubation was continued for 1 hr, and viruses released from the cells were harvested at 240 min for a plaque assay (*see* text). The bars at right marked '*PFU*' represent PFUs per well.

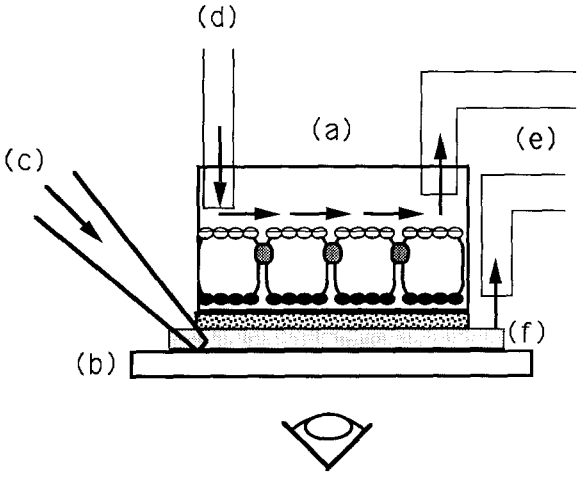

Fig. 2. The perfusion chamber used for fluorescence measurements of polarized MDCK cells. A 3.0-μm pore size polycarbonate filter held in a 6.5-mm diameter Costar Transwell insert (*a*) was placed on top of two, 20-μm thick flat glass capillaries (*f*) that ran parallel to one another, about 5.5 mm apart, on a number 0 coverslip (*b*). Buffer was perfused past the basal-lateral surface at 0.2 ml min^{-1} from a borosilicate glass pipette (*c*) whose 20-μm diameter tip was placed between the glass capillaries and beneath the base of the Transwell insert. Buffer was perfused over the apical surface at the same rate from a Teflon tube (*d*) placed directly over cells in the field of view. Buffer was removed from each compartment by a sipper across the monolayer from each perfusion source (*e*). The cells were viewed through the polycarbonate filter by an oil immersion lense on an inverted microscope.

ment of cytosol fluorophores through a polycarbonate filter—it was necessary to establish that our data accurately represent the state of cells in the monolayer before testing hypotheses. Figure 3 shows an assay in which BCECF-loaded cells were pulsed with 10 mM acetate at pH 6.0. Many weak acids rapidly permeate biological membranes and thereby acidify cytosol (Roos & Boron, 1981). In Fig. 3, acetic acid dropped the 495/440-nm fluorescence ratio of BCECF to a new steady state within 2 min. This is equivalent to a cytosol pH shift from 7.3 to 6.4. Removal of acetate caused a rapid rise in pH*c*, including a transient alkaline spike that gradually dropped back to normal as observed previously in mouse macrophages and chick fibroblasts (Heuser, 1989*a*). To establish that the dye was intracellular and not occluded between the basal and polycarbonate membranes, we first pulsed with pH 6.0 buffer followed by pH 6.0 buffer plus acetate (Fig. 4). Acidification of the external buffer without acetate caused some drop in the 495/440-nm ratio. This could be explained either by BCECF trapped outside of the cells or by a true drop in pH*c* which lags 0.5–1.0 units behind external pH in many cells (Heuser, 1989*b*), including MDCK cells (Oberleither et al., 1989). By comparison, the additional abrupt drop in the 495/440-nm ratio upon acetate addition can only be explained by acetic acid permeation into cytosol and titration of intracellular BCECF. A similar experiment with ionomycin-loaded MDCK cells gave the anticipated response of intracellular Fura-2 to high and low extracellular Ca^{2+} (Fig. 5). We conclude that fluorescence measurements performed using the chamber in Fig. 2 accurately report

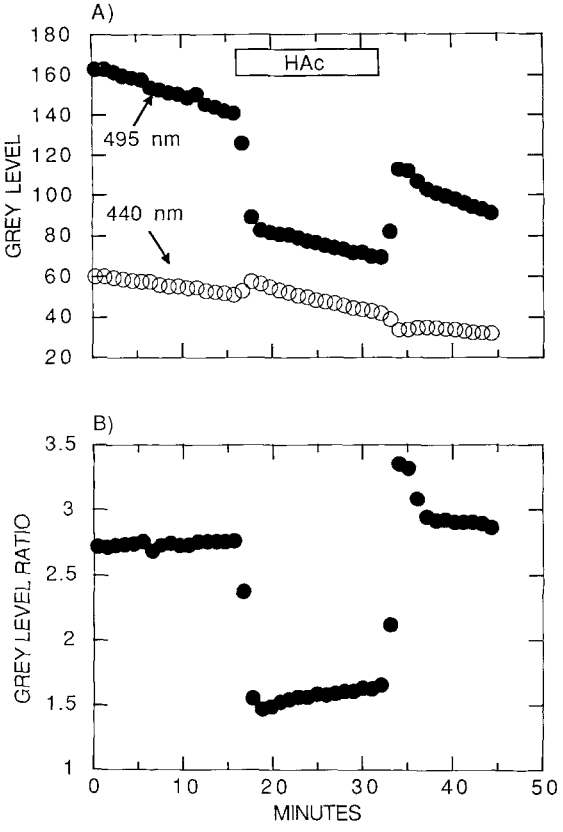

Fig. 3. The response of MDCK cells to extracellular acetate as measured by BCECF fluorescence. Cells in a confluent monolayer atop a translucent polycarbonate filter were preloaded with BCECF-AM as described in the text. The filter was placed onto the microscope as diagrammed in Fig. 2 and perfused, both apically and basally, at 0.2 ml min^{-1} with buffer A. The excitation light wavelength was alternated between 495 and 440 nm; emitted light was measured at 535-nm wavelength. At 16 min, the apical and basal perfusates were simultaneously switched to buffer A supplemented with 10 mM acetate at pH 6.0 ('*HAc*'). They were switched back to buffer A at 32 min. (*A*) Change in grey level (light intensity) at the two excitation frequencies in response to acetate addition. (*B*) The ratio of emitted light intensities at the two excitation frequencies shown in *a*. The steady-state intracellular pH from 0–15 min was 7.3 based on a calibration procedure described in the text. This value is intermediate between previous measurements for MDCK cells at 0% CO_2 (pH 7.5; Selvaggio et al., 1986) and 5% CO_2 (pH 7.1; Kurtz & Golchini, 1987). Addition of acetate dropped the apparent intracellular pH to 6.4. All buffers in this experiment and others with BCECF or Fura-2 contained 250 μM sulfinpyrazone to block unloading of entrapped dye by organic anion pumps. Sulfinpyrazone had no effect on VSV infection of MDCK cells, whereas the more widely used blocker (probenecid) markedly reduced infection measured by a plaque assay (*data not shown*).

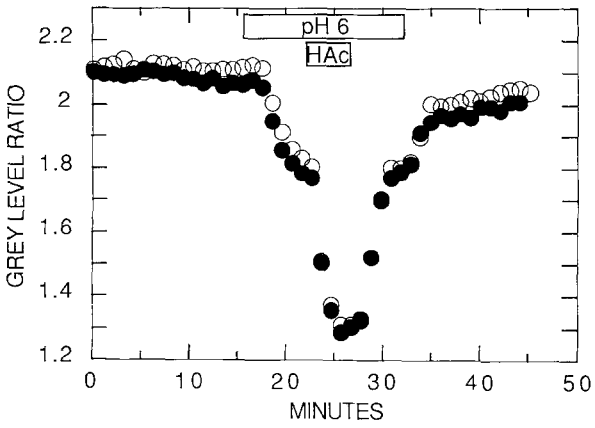

Fig. 4. The separate effects of pH 6 buffer and pH 6 buffer plus 10 mM acetate upon BCECF fluorescence in MDCK cells. Grey level ratio in this figure has the same meaning as in Fig. 3b. From 0–16 min, the MDCK cell monolayer was perfused apically and basally at 0.2 ml min^{-1} with buffer A at pH 7.4. At 16 min, the perfusate was switched to buffer A at pH 6.0. This was followed at 22 min by pH 6.0 buffer A plus 10 mM acetate. The sequence of additions was reversed beginning at 26 min.

significant physiological changes in cell cytosol on the time scale of seconds to minutes.

Because this report focuses on electrical potential across the plasma membrane of MDCK cells, one specific requirement was to establish a reliable fluorometric test for plasma membrane potential shifts. Anionic bis-oxonols are relatively nontoxic potential-sensitive dyes that slowly accumulate in cytosol upon membrane depolarization. One of these is $DiBAC(4)_3^-$. In rat mammary tumor cells and mouse embryo cells, $DiBAC(4)_3^-$ binds to cytoplasm proteins and gives a 1% change in fluorescence per millivolt change in plasma membrane potential (Bräuner, Hülser & Strasser, 1984). Figure 6*a* shows $DiBAC(4)_3^-$-loaded MDCK cells viewed through a polycarbonate filter as diagrammed in Fig. 2; Fig. 6*b* shows cells under the same condition viewed from the apical side on a filter that was cutout and inverted on the microscope. In both cases, a bright signal was emitted from dye associated with the periphery of the cytoplasm which clearly delineated cell boundaries, although some detail was obscured by the filter. We found that this dye responded as expected to depolarizing or hyperpolarizing media. For instance, Table 1 lists conditions that evoke known membrane potential shifts in MDCK cells (Paulmichl et al., 1985; Jungwirth, Lang & Paulmichl, 1989) along with changes in $DiBAC(4)_3^-$ fluorescence that we measured in the high resistance MDCK strain. An example is shown in Fig. 7. In all cases, the direction and size of the fluorescence shift was consistent with the apparent change in membrane potential. We conclude that $DiBAC(4)_3^-$ is a reliable semi-quantitative indicator of membrane potential in polarized MDCK cells.

Table 1. The correlation between changes in plasma membrane potential of MDCK cells and changes in $DiBAC(4)_3^-$ fluorescence induced by various solutes

Solute	$\delta\Delta\Psi_{pm}$ (mV)	ROI (n)	$\Delta F/F_o$ mean ± SD	% Change in fluorescence (per mV)
10 μM ATP	−18	2	−0.20 ± 0.00	−1.1
1 mM $BaCl_2$	+20	5	+0.20 ± 0.03	+1.0
35 mM K^+	+24	2	+0.21 ± 0.05	+0.9

The resting plasma membrane potential ($\Delta\Psi_{pm}$) in MDCK cells is about −50 mV (inside negative) (Paulmichl et al., 1985). $\delta\Delta\Psi_{pm}$ represents the shift in plasma membrane potential measured elsewhere (Paulmichl et al., 1985; Jungwirth et al., 1989) using microelectrodes inserted into subconfluent MDCK cells on glass coverslips. ΔF is the change in $DiBAC(4)_3^-$ fluorescence of polarized high resistance MDCK cells relative to baseline fluorescence (F_0) measured in this study. The last column (% change in fluorescence per mV change in plasma membrane potential) is $(\Delta F/F_0 \div \delta\Delta\Psi_{pm}) \cdot 100$. Fluorescence measurements were made on regions of interest (ROI) composed of ten cells each.

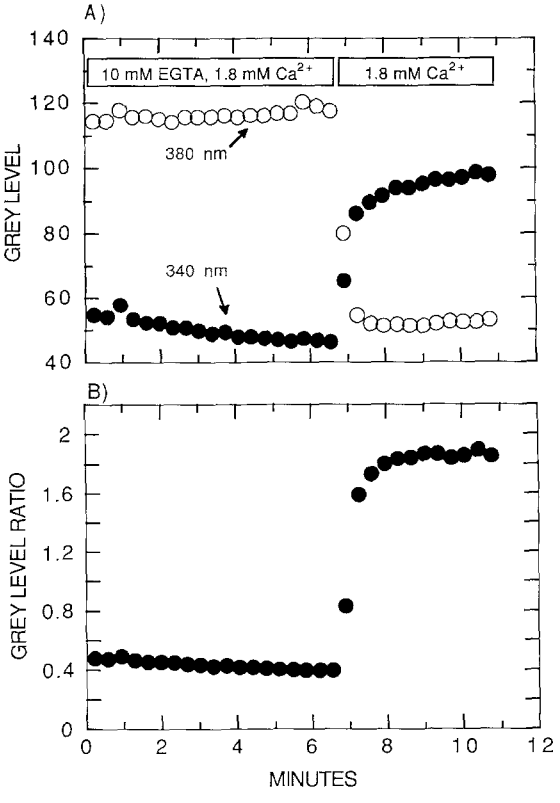

Fig. 5. The response of Fura-2-loaded MDCK cells to high and low levels of intracellular Ca^{2+}. Cells were preloaded with Fura-2-AM as described in the text. They were then incubated in 5 μM ionomycin for 2 min and placed onto the microscope as in Fig. 2. Emitted light intensity (510 nm) was measured pixel by pixel at each of two excitation frequencies (340 and 380 nm), and the grey level ratio was calculated from F_{340}/F_{380}. From 0 to 7 min, the cells were perfused at 0.2 ml min^{-1} (apical and basal) with buffer A containing 10 mM EGTA and 1.8 mM Ca^{2+} (zero free Ca^{2+}), followed by buffer A with 1.8 mM Ca^{2+} from 7 to 11 min. (*A*) The average fluorescent output (grey level) for a single cell at the two separate excitation frequencies. (*B*) The average grey level ratio (F_{340}/F_{380}) for the same cell. Six out of six cells gave the same qualitative response as the cell shown here, although the maximum grey level ratio varied between 1.6 and 2.2.

High K^+ in the Basal-Lateral Medium Reduces the Plasma Membrane Potential in MDCK Cells and Inhibits VSV Infection; High K^+ in the Apical Medium Has No Effect

Could plasma membrane depolarization in high K^+ buffer explain the observed inhibition of virus infection? K^+ permeation of polarized MDCK cells occurs primarily through the basal-lateral membrane (Aiton et al., 1982). On this basis it is generally inferred that K^+ mediates plasma membrane potential at the basal-lateral membrane; however, the inference has never been tested directly. We undertook such an experiment using highly resistant monolayers of MDCK cells which permitted independent perfusion of apical and basal-lateral membranes. Figure 8 shows that high K^+ buffer applied to the basal-lateral membrane reversibly diminished the electrical potential in MDCK cells (increasing fluorescence). The same buffer applied to the apical side had little or no effect. This outcome agrees with the conventional model and predicts that if high K^+ inhibits acid-processed virus infection through its effect on $\Delta\Psi_{pm}$, then the inhibition should only be observed at the basal-lateral membrane.

We tested this prediction using an infection assay. Generally, VSV virions began to bud from control MDCK monolayers at 4–5 hr post-infection (Fig. 9). Early, simultaneous application of high K^+ buffer to the apical and basal-lateral surfaces delayed virion release by one or more hours with full recovery to control rates by 8.5 hr post-infection. Thus, high K^+ applied following endocytosis reversibly inhibited VSV infection of polarized MDCK cells as was true for BHK cells. This effect was concentration dependent (Table 2,*A*). Application of high K^+ buffer to the basal-lateral surface alone resulted in the same level of inhibition (Table 2,*A*);

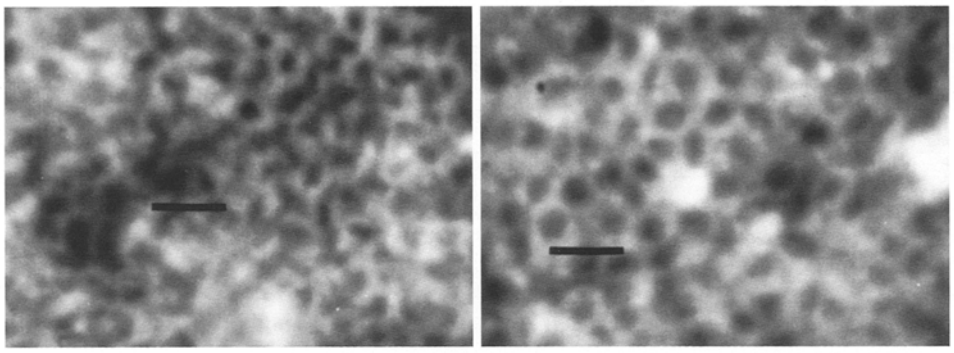

Fig. 6. A monolayer of DiBAC(4)$_3^-$-loaded MDCK cells viewed with and without a polycarbonate filter between the monolayer and the microscope objective. Cells were loaded with DiBAC(4)$_3^-$ as described in the text. The bath contained buffer A plus 2 μM DiBAC(4)$_3^-$ at 34°C with a 1% CO_2 atmosphere. (*A*) View of a monolayer through a 3.0-μm pore size polycarbonate filter as diagrammed in Fig. 2. (*B*) Direct view of the same monolayer without the filter in the light path which was achieved by cutting out the filter and inverting it onto the glass coverslip. Each image is an average of eight frames taken of a field where the excitation light frequency was 495 nm and the emission frequency was 535 nm. The bar represents 20 μm.

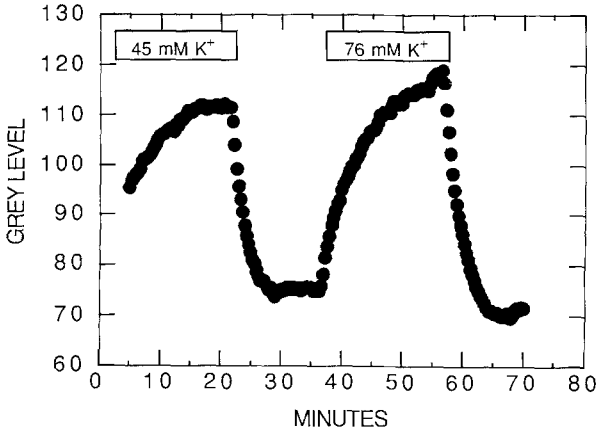

Fig. 7. The response of DiBAC(4)$_3^-$-loaded MDCK cells to high levels of basal-lateral K^+. Fluorescent light (495-nm excitation wavelength, 535-nm emission wavelength) was acquired and averaged as described in the text. The apical surface was perfused throughout this experiment with buffer A at 0.2 ml min^{-1}. The basal-lateral surface was perfused at the same rate with buffer A containing: 45 mM K^+ and 90 mM Na^+ (0–20 min), standard buffer A with 5 mM K^+ and 130 mM Na^+ (20–38 min), buffer A plus 76 mM K^+ and 59 mM Na^+ (38–58 min), and standard buffer A (58–70 min). In this figure, grey level represents the average 495-nm wavelength light intensity for a group of 10 cells. A separate group of 10 cells on the same monolayer gave essentially the same response, as did individual cells in separate experiments. The initial cycle in this experiment (basal-lateral perfusion with buffer A plus 45 mM K^+ for 20 min followed by standard buffer A for 20 min) constitutes the DiBAC(4)$_3^-$ preloading regime used in this study. Without the high K^+ pulse, the baseline fluorescent light intensity drifted upward for as much as 2 hr. DiBAC(4)$_3^-$ concentration in the medium was 2 μM throughout this and all similar experiments.

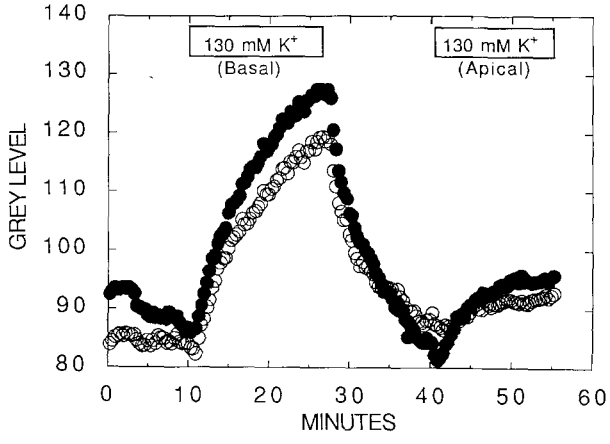

Fig. 8. Changes in $\Delta\Psi_{pm}$ of MDCK cells in response to 130 mM K^+ applied to the apical or basal-lateral surfaces of a high resistance monolayer. The protocols for preloading the cells with DiBAC(4)$_3^-$ and acquiring fluorescent light intensities are described in the text. From 0–10 min, both the apical and basal-lateral surfaces were perfused with buffer A at 0.2 ml min^{-1}. At 10–27 min, the basal-lateral perfusate was switched to buffer A modified with 130 mM K^+ and 5 mM Na^+ and then returned to standard buffer A (27–40 min). At 40 min, the apical perfusate was changed to 130 mM K^+ buffer. Each set of data shown in this figure represents the average 495-nm light intensity for pixels selected within the cytoplasm of a single cell. The open circles were typical of most cells in that high K^+ applied to the basal-lateral membrane induced a large increase of light intensity (indicative of plasma membrane depolarization) while the same high K^+ buffer had little effect when applied apically. The filled circles represent a less common case where apical high K^+ had a small but measurable effect on light intensity. The latter case was generally found in monolayers with resistances at the low end of the range used (ca. 500 Ω cm^{-2}). An experiment in which 130 mM K^+ buffer was added to the apical membrane first and the basal-lateral membrane second gave the same relative response as shown here.

Table 2. The dependence of VSV production upon external [K^+], ATP, and Ba^{2+}.

Treatment	Incubation period	PFU hr^{-1}		Control/treatment
	Hours post-infection	Control	Treatment	
		[A]		
135 mM K^+, apical and basal	4–5	24	0	24/0
	5–6	480	6	80/1
76 mM K^+, apical and basal	3–4	72	6	12/1
	4–5	4800	1200	4/1
45 mM K^+, apical and basal	3–4	72	18	4/1
	4–5	4800	900	5/1
135 mM K^+, apical only	4–5	54	54	1/1
	5–6	450	420	1/1
135 mM K^+, basal only	4–5	54	0	54/0
	5–6	450	12	37/1
		[B]		
1 mM $BaCl_2$, basal only	3–4	240	24	10/1
	4–5	3000	720	4/1
135 mM K^+, basal, pH 7.1	4–5	300	n.d.	n.d.
	5–6	2400	30	80/1
Control + 1 mM ATP, apical	3–4	240	200 ± 6	1/1
	4–5	3900 ± 1230	6750 ± 210	0.5/1
	5–6	10,050 ± 4030	9600 ± 5090	1/1

High resistance MDCK cells were exposed to the treatments at left for 155 min, after which virus production (PFU hr^{-1}) was measured (*see* text). The first hour shown for each treatment represents the time in which virions first appeared in the basal medium of the control, followed by the next time point harvested. PFU ± SD are for replicates within the same experiment where plaque assays were performed on separate days. Total cell protein synthesis was relatively unaffected during a 5-hr exposure to 135 mM K^+ which dropped ^{14}C-leucine incorporation to 65% of control. n.d. = not done.

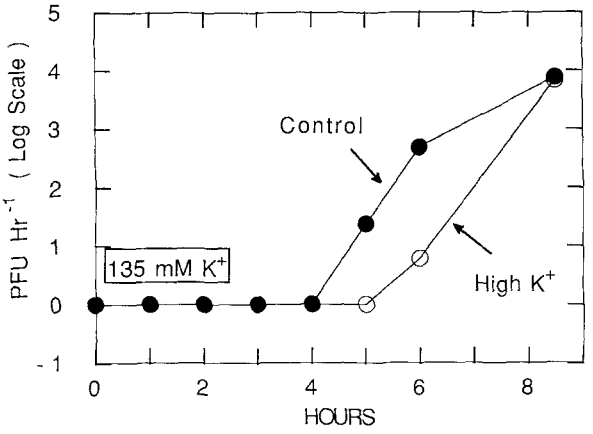

Fig. 9. The inhibitory effect of high K^+ buffer on VSV infection of MDCK cells, and recovery of infectivity over time. The experimental protocol is described in the text. Following endocytosis, the apical and basal-lateral surfaces of MDCK monolayers were incubated for 160 min in either standard buffer A containing 5 mM K^+ and 130 mM Na^+ (filled circles) or buffer A modified with 135 mM K^+ (open circles). At 160 min, the cells were rinsed and placed into wells containing standard buffer A. After 1 hr, aliquots were taken from the basal-lateral side of each monolayer and tested for newly synthesized virions by a plaque assay (*see* text). Each monolayer was then transferred to fresh buffer A and allowed to incubate for another hour when the plaque assay was performed again. This series of steps was repeated up to 6 hr post-infection. One final incubation step was performed from 6 to 8.5 hr.

by comparison, the highest K^+ level (135 mM) applied to the apical membrane did not inhibit infection (Table 2,*A*).

1 mM $BaCl_2$ in Basal-Lateral Perfusate Diminishes the Plasma Membrane Potential in MDCK Cells and Inhibits VSV Infection

To this point, our experiments have demonstrated membrane depolarization and VSV inhibition by high K^+ media without determining a mechanism. The most likely possibility is that high external K^+ diminishes the K^+ concentration gradient responsible for generating a diffusion potential by K^+ efflux through basal-lateral channels. To test this, we added 1 mM $BaCl_2$ (in the absence of $NaHCO_3$) to the basal-lateral surface of several monolayers. Ba^{2+} is known to block K^+ channels and depolarize subconfluent MDCK cells on glass coverslips (Paulmichl et al., 1985). Our own data (Table 1) indicate that basal-lateral Ba^{2+} decreases the plasma membrane potential in polarized MDCK cells. Thus, we predicted that Ba^{2+} applied to the basal surface would inhibit VSV infection if K^+ diffusion through basal-lateral channels were required for infection. We found that 1 mM basal-lateral Ba^{2+} did signifi-

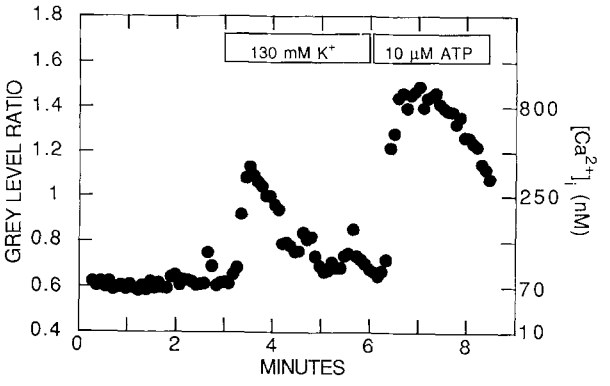

Fig. 10. The effect of high extracellular K^+ and ATP on cytosol free Ca^{2+} in MDCK cells. MDCK monolayers on polycarbonate filters were preloaded with Fura-2-AM as described in the text. The apical and basal-lateral surfaces were initially perfused at 0.2 ml min^{-1}. The basal-lateral perfusate was changed to buffer A modified with 130 mM K^+ at 3 min, then to buffer A containing 10 μM ATP at 6 min. The data shown here represent the average grey level ratio (F_{340}/F_{380}) for pixels within a single cell (y-axis at left) and the approximate free Ca^{2+} concentration associated with those ratios calculated with the equation (y-axis at right). (For a review of the pitfalls associated with intracellular Ca^{2+} calibration, *see* Roe, LeMasters and Herman (1990)). In five of five cells assayed in this experiment, high basal-lateral K^+ and 10 μM basal-lateral ATP caused increases of $[Ca^{2+}]_i$ similar to that shown here. In a separate experiment, ATP added apically had essentially the same effect as ATP added basally.

cantly inhibit VSV infection (Table 2,*B*) in support of the postulate.

Shifts in Cytosol Ca^2 and pH Cannot Explain VSV Inhibition

One possible way in which plasma membrane depolarization could inhibit infection is by inducing a change in the cytosol activity of a regulatory ion (e.g., Ca^{2+} or H^+). For instance, plasma membrane depolarization is known to induce transient or sustained increases in resting cytosol Ca^{2+} of some excitable (Connor, Tseng & Hockberger, 1987; Fatatis & Russell, 1991) and nonexcitable cells (Harootunian, Kao & Tsien, 1988).

We, therefore, tested the effect of high extracellular K^+ upon resting cytosol Ca^{2+} concentration and cytosol pH. We found that 130 mM K^+ medium caused an increase in $[Ca^{2+}]_i$ from about 50 to about 300 nM (Fig. 10). The increase was not sustained and returned to 50 nM within 3 min. We then asked if the observed $[Ca^{2+}]_i$ spike could account for inhibition of VSV infection. To test this, we measured VSV infection of MDCK cells in the presence of extracellular ATP. ATP *hyper*polarizes MDCK cells (Table 1) and induces a rise in cytosol Ca^{2+} that is larger than that induced by 130 mM K^+ whether applied basally or apically (Fig. 10). We found that 1 mM ATP applied apically had no effect on VSV infection of MDCK cells (Table 2,*B*); therefore, a rise in resting cytosol Ca^{2+} alone cannot account for VSV inhibition.

High K^+ medium applied to the basal-lateral membrane also induced a modest alkalinization of cytosol pH in some cells from the normal value of pH 7.3–7.4 to pH 7.5–7.6 (Fig. 11*A*). To determine if this alkalinization could account for VSV inhibition by high K^+, we ran a plaque assay in 135 mM K^+ buffer A at pH 7.1, wherein pH_i remained fixed at its normal value during depolarization (Fig. 11*B*). We found that 135 mM basal K^+ still dramatically inhibited VSV production (Table 2,*B*); therefore, the inhibitory step is not pH related.

Discussion

Our results demonstrate that high K^+ buffer inhibited VSV infection of BHK and MDCK cells. In agreement with experiments on SFV (Helenius et al., 1985), inhibition of VSV production occurs primarily at an early step following endocytosis.

Helenius et al. (1985) proposed that the cause of inhibition is plasma membrane depolarization. This report supports that postulate based on two tests. First, high K^+ buffer applied to the basal-lateral membrane of MDCK cells in tight monolayers blocked infection (Table 2,*A*) and diminished $\Delta\Psi_{pm}$(Fig. 8), while high K^+ buffer applied apically had no effect on either VSV infection or on membrane potential. This result is reasonable because K^+ permeates MDCK cells mostly through the basal-lateral membrane; therefore, its contribution to membrane potential would only be modified at that membrane. Our second test showed that 1 mM Ba^{2+} applied basally could also block VSV infection of MDCK cells at a level similar to inhibition by 76 mM extracellular K^+ (Table 2,*B*). Ba^{2+} is known to block K^+ channels and induces an 18-mV depolarization in MDCK II cells (Paulmichl et al., 1985). Therefore, the observed inhibition of VSV is consistent with the postulate.

A molecular mechanism linking plasma membrane depolarization to inhibition of SFV and VSV production has not been demonstrated to date. Possibilities can be rigorously limited to the three ways in which cells use $\Delta\Psi_{pm}$ for cell function: (i) electrical work in which charge transfer through a potential difference is used to transport a solute against an electrochemical gradient; (ii) as a component of total electrochemical potential of a charged solute across

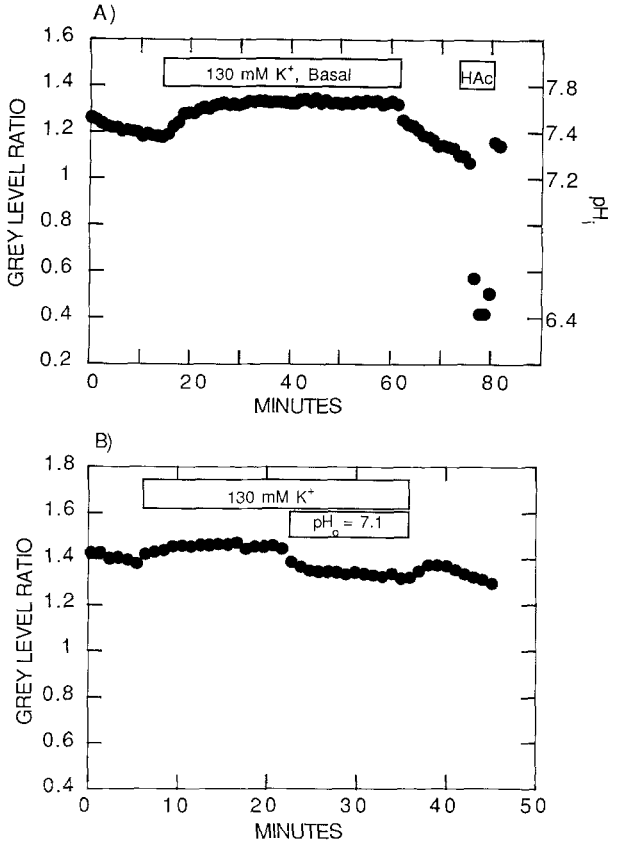

Fig. 11. The effect of high K^+ buffer on intracellular pH of MDCK cells. Cells were preloaded with BCECF-AM as described in the text. Emitted light was measured at 535-nm wavelength for two excitation wavelengths (495 and 440 nm). The data presented here represent average F_{495}/F_{440} ratios among pixels within a single cell. (*A*) The MDCK monolayer was initially perfused across the apical and basal surfaces at 0.2 ml min^{-1} with buffer A. The basal-lateral perfusate was switched to buffer A containing 130 mM K^+ at 14 min, then back to standard buffer A at 60 min. A short pulse of 10 mM acetate in buffer A at pH 6.0 was delivered to the basal-lateral surface (74–79 min), then changed back to the control buffer for the last 4 min of the run. In this experiment, five of five cells showed alkalinization upon high K^+ addition similar to the cell shown, with an average change of +0.2 pH units. In another experiment, only four of six cells indicated cytosol alkalinization, and the effect was less pronounced (+0.1 pH units). (*B*) In this experiment, the monolayer was initially perfused apically and basally with buffer A as above. The basal-lateral perfusate was switched to 130 mM K^+ buffer A at 6 min, and then to the same buffer titrated to pH 7.1 at 22 min. Finally, this was displaced by standard buffer A at 35 min. In six of six cells measured, acidification of the high K^+ buffer to pH 7.1 reversed any intracellular alkalinization induced by high K^+ at pH 7.4.

the plasma membrane, which renders a reaction spontaneous; and (iii) as an electric field which aligns or moves dipoles within the field (e.g., the positively charged intra-membrane S4 segments of voltage-sensitive Na^+ and Ca^{2+} channels (Jan & Jan, 1989)). Any other mechanism that may directly block virus infection—for example inhibition of fusion between viral and endosomal membranes (Helenius et al., 1985)—must be triggered by one of these if $\Delta\Psi_{pm}$ plays a central role as our data suggest.

One possible 'trigger' that we considered in this study was an increase of cytosol Ca^{2+} caused by plasma membrane depolarization. We found that 130 mM K^+ induced a transient $[Ca^{2+}]$ increase in MDCK cells that fell back to baseline within minutes (Fig. 10). In excitable cells, the plasma membrane contributes to regulation of $[Ca^{2+}]_i$ by Ca ATPases and Na^+/Ca^{2+} exchangers (Strehler, 1990), voltage-gated Ca^{2+} channels (Jan & Jan, 1989), and by hydrolysis of phosphatidyl inositols to second messengers (Berridge & Irvine, 1989). To our knowledge, there is no evidence in any cell type that depolarization can directly induce phosphatidyl inositol hydrolysis to inositol phosphates. By comparison, both the gated channels (Jan & Jan, 1989) and Na^+/Ca^{2+} exchangers (Strehler, 1990) are voltage dependent and contribute to increased cytosol Ca^{2+} in excitable cells upon plasma membrane depolarization. Na^+/Ca^{2+} exchangers are thought to be common in non-excitable cells (Strehler, 1990), and voltage-gated Ca^{2+} channels have been reported in at least one nonexcitable cell, rat embryo fibroblasts (Harootunian et al., 1988). Thus, our working hypothesis is that one or both of these proteins exist in the plasma membrane of MDCK cells and is responsible for the Ca^{2+} spike we observed.

A $[Ca^{2+}]_i$ increase alone cannot account for inhibition of virus production in high K^+ media because a similar $[Ca^{2+}]_i$ change induced by ATP did not alter VSV infection (Table 2,*B*). This experiment cannot exclude the possibility that depolarization activated other second messengers which we did not measure such as inositol 1,4,5-tris-phosphate (Berridge & Irvine, 1989).

Cytosol pH affects numerous processes in cells, including VSV-G-protein transport from the *trans*-Golgi network to the cell surface (Cosson et al., 1989) and microtubule-dependent movement and shape of lysosomes (Heuser, 1989*a*). In MDCK cells, Na^+/H^+ exchange regulates against acid-loading (Selvaggio et al., 1986), and Cl^-/HCO_3^- exchange regulates against alkalosis (Kurtz & Golchini, 1987). Both exchangers are located in the apical membrane (Oberleither et al., 1989). We reasoned that if either of these mechanisms were sensitive to electrical potential, or if cytosol pH were influenced by the protonic Nernst potential, then depolarization by high K^+ at the basal-lateral membrane could induce a significant shift in cytosol pH. We found that pH_i did increase by 0.1–0.2 pH units during the high K^+ treatment (Fig. 11). However, this modest pH shift does not contribute to VSV

inhibition because control of pH_i at a normal value does not alleviate inhibition by depolarization.

An alternative mechanism that we are currently testing is that depolarization blocks translocation of the viral nucleocapsid across the epithelial cell plasma membrane. There are numerous precedents for $\Delta\Psi_{pm}$-dependent protein translocation across biological membranes including the *trans*-membrane transfer of the voltage-gating segment of the bactericidal protein colicin E1 (Merrill & Cramer, 1990; Abrams et al., 1991), import of protein precursors into mitochondria using general insertion proteins (Miller & Cumsky, 1991), and transport of proteins from cytoplasm to periplasm in *E. coli* using translocase (Schiebel et al., 1991). For this mechanism to operate in VSV infection, the nucleocapsid—or a component of the nucleocapsid—would have to associate with the plasma membrane following endocytosis. This could be accomplished by recycling of the virus receptor-virus complex back to the plasma membrane following acid processing. A similar step has been postulated to explain $\Delta\Psi_{pm}$ dependence of diphtheria toxin intoxication (Hudson et al., 1988).

We thank Kenneth Spring for many helpful discussions concerning fluorescence digitized imaging systems, James Russell for his collaboration in the design of our imaging system, Herbert Chase for suggestions on dye loading into MDCK cells, and Manfred Schubert and George Harmison for providing expertise on VSV.

References

Abrams, C.K., Jakes, K.S., Finkelstein, A., Slatin, S.L. 1991. Voltage-dependent gating of colicin E1 is associated with membrane translocation of a segment of the protein. *Biophys J.* **59:**458*a*

Aiton, J.F., Brown, C.D.A., Ogden, P., Simmons, N.L. 1982. K^+ transport in "tight" epithelial monolayers of MDCK cells. *J. Membrane Biol.* **65:**99–109

Berridge, M.J., Irvine, R.F. 1989. Inositol phosphates and cell signaling. *Nature* **341:**197–205

Bräuner, T., Hülser, D.F., Strasser, R.J. 1984. Comparative measurements of membrane potentials with microelectrodes and voltage-sensitive dyes. *Biochim. Biophys. Acta* **771:**208–216

Connor, J. A., Tseng, H.-Y., Hockberger, P.E. 1987. Depolarization- and transmitter-induced changes in intracellular Ca^{2+} of rat cerebellar granule cells in explant cultures. *J. Neurosci.* **7:**1384–1400

Cosson, P., de Curtis, I., Pouysségur, J., Griffiths, G., Davoust, J. 1989. Low cytoplasmic pH inhibits endocytosis and transport from the *trans*-Golgi network to the cell surface. *J. Cell Biol.* **108:**377–387

Di Virgilio, F., Steinberg, T.H., Silverstein, S.C. 1990. Inhibition of Fura-2 sequestration and secretion with organic anion transport blockers. *Cell Calcium* **11:**57–62

Fatatis, A., Russell, J.T. 1991. Spontaneous changes in intracellular calcium concentration in type I astrocytes from rat cerebral cortex in primary culture. *Glia (in press).*

Grynkiewicz, G., Poenie, M., Tsien, R.Y. 1985. A new generation of Ca^{2+} indicators with greatly improved fluorescence properties. *J. Biol. Chem.* **260:**3440–3450

Harootunian, A.T., Kao, J.P.Y., Tsien, R.Y. 1988. Agonist-induced calcium oscillations in depolarized fibroblasts and their manipulation by photoreleased $Ins(1,4,5)P_3$, Ca^{2+}, and Ca^{2+} buffer. *Cold Spring Harbor Symp. Quant. Biol.* **53:**945–953

Helenius, A., Kielian, M., Wellsteed, J., Mellman, I., Rudnick, G. 1985. Effects of monovalent cations on Semliki Forest virus entry into BHK-21 cells. *J. Biol. Chem.* **260:**5691–5697

Heuser, J. 1989*a*. Changes in lysosome shape and distribution correlated with changes in cytoplasmic pH. *J. Cell Biol.* **108:**855–864

Heuser, J. 1989*b*. Effects of cytoplasmic acidification on clathrin lattice morphology. *J. Cell Biol.* **108:**401–411

Hudson, T.H., Scharff, J., Kimak, M.A.G., Neville, D.M., Jr. 1988. Energy requirements for diphtheria toxin translocation are coupled to the maintenance of a plasma membrane potential and a proton gradient. *J. Biol. Chem.* **263:**4773–4781

Jan, L.Y., Jan, Y.N. 1989. Voltage-sensitive ion channels. *Cell* **56:**13–25

Jungwirth, A., Lang, F., Paulmichl, M. 1989. Effect of extracellular adenosine triphosphate on electrical properties of subconfluent Madin-Darby canine kidney cells. *J. Physiol.* **408:**333–343

Kurtz, I., Golchini, K. 1987. Na^+-independent Cl^--HCO_3^- exchange in Madin-Darby canine kidney cells. *J. Biol. Chem.* **262:**4516–4520

Marsh, M., Helenius, A. 1989. Virus entry into animal cells. *Adv. Virus Res.* **36:**107–151

Merrill, A.R., Cramer, W.A. 1990. Identification of a voltage-responsive segment of the potential-gated colicin E1 ion channel. *Biochemistry* **29:**8529–8534

Miller, B.R., Cumsky, M.G. 1991. An unusual mitochondrial import pathway for the precursor to yeast cytochrome *c* oxidase subunit Va. *J. Cell Biol.* **112:**833–841

Oberleither, H., Kersting, U., Silbernagl, S., Steigner, W., Vogel, U. 1989. Fusion of cultured dog kidney (MDCK) cells: II. Relationship between cell pH and K^+ conductance in response to aldosterone, *J. Membrane Biol.* **111:**49–56

Paulmichl, M., Gstraunthaler, G., Lang, F. 1985. Electrical properties of Madin-Darby canine kidney cells: Effects of extracellular potassium and bicarbonate. *Pfluegers Arch.* **405:**102–107

Roe, M.W., LeMasters, J.J., Herman, B. 1990. Assessment of Fura-2 for measurements of cytosolic free calcium. *Cell Calcium* **11:**63–73

Roos, A., Boron, W.F. 1981. Intracellular pH. *Physiol. Rev.* **61:**296–434

Schiebel, E., Driessen, A.J.M., Hartl, F.-U., Wickner, W. 1991. $\Delta\mu H^+$ and ATP function at different steps of the catalytic cyclic of preprotein translocase. *Cell* **64:**927–939

Selvaggio, A.M., Schwartz, J.H., Bengele, H.H., Alexander, E.A. 1986. Kinetics of the Na^+-H^+ antiporter as assessed by the change in intracellular pH in MDCK cells. *Am. J. Physiol.* **251:**C558–C562

Strehler, E.E. 1990. Plasma membrane Ca^{2+} pumps and Na^+/Ca^{2+} exchangers. *Semin. Cell. Biol.* **1:**283–295

Wiley, D.C., Skehel, J.J. 1987. The structure and function of the hemagglutinin membrane glycoprotein of influenza virus. *Annu. Rev. Biochem.* **56:**365–394

Received 8 May 1991; revised 12 July 1991